Chapter ?

©Saxe-Coburg Publications, 2010.
Developments and Applications in
Computational Structures Technology
B.H.V. Topping, J.M. Adam, F.J. Pallarés
R. Bru and M.L. Romero, (Editors)
Saxe-Coburg Publications, Stirlingshire, Scotland, 888-888.

Recent Advances in Global-Local Multiscale Methods for Computational Mechanics

S. De and Rahul
Advanced Computational Research Laboratory
Department of Mechanical, Aerospace and Nuclear Engineering
Rensselaer Polytechnic Institute
Troy NY, United States of America

Abstract

The objective of multiscale modeling is to predict the response of complex systems at all relevant spatial and temporal scales at a cost that is sub-linear with respect to the full micro-scale solver [1]. Scale linking is currently performed using hierarchical [2] and concurrent [3-9] schemes. This global-local type of multiscale methods [10-20] falls within the category of hierarchical multiscale methods where the stress-strain relationship at every integration point of the macro-scale is computed by suitably deforming an associated representative volume element (RVE). The major advantage of this class of methods is the ability to model arbitrary nonlinearities at the micro-scale as no *a priori* constitutive assumption is made at the macro-scale. In this chapter we will summarize implicit and explicit global-local multiscale methods, their current developments, challenges and applications to computational mechanics.

Keywords: multiscale modeling, hierarchical multiscale, global-local method, Jacobian-free Newton-Krylov, preconditioner, massively parallel systems.

1 Introduction

Most biological and engineering materials are heterogeneous at certain length scales and this heterogeneity has significant impact on the macroscopic material response. For instance, most engineering metals and alloys are polycrystalline with grains of various orientations. Second phase inclusions and voids add to this heterogeneity. Advanced forming processes force a material to undergo complex loading paths leading to evolution of the microstructure. Furthermore, due to the ongoing trend towards miniaturization of devices, the microstructure is no longer negligible compared to the component size, giving rise to so-called "size effects". Composites are another class of engineering materials which are highly heterogeneous. The emergence of nanostructured composites with carbon nanotubes or nanoparticle

fillers has opened up the unique possibility of controlling properties at the molecular level where, due to the very high interfacial area, the properties of the polymer matrix are essentially controlled by the interaction between the chain and the nanoscale filler. The enhanced properties such as low weight and high energy absorption of metal foams arise primarily from their cellular microstructure.

In order to create materials, devices, and systems as the basis for new products and industries, engineers must learn to model and design at the macroscopic scale taking into account the relevant micro structural features. A full-scale finite element analysis of these systems is out of question, so is the possibility of more accurate but computationally demanding atomistic or *ab initio* techniques. Hence, robust and reliable multiscale computational strategies are essential to overcome the "tyranny of scales".

The goal of multiscale modeling is to take into account the interconnectivity of the essential phenomena occurring at multiple length and time scales preserving macroscopic conservation principles. The objective of recent multiscale methods, which distinguishe them from traditional ones such as multigrid, wavelet, fast multipole or adaptive mesh refinement techniques, is to capture the macroscale behavior with a cost which is sublinear compared to the cost of a full microscale solver. Scale linking is performed using hierarchical, concurrent or a combination of these schemes. Examples of concurrent coupling methods [3-9] are hybrid atomistic-continuum techniques in which spatial regions subjected to large local field variations (such as dislocations or cracks) are represented atomistically, while the rest of the model is continuum [3-9]. For the simulation of heterogeneous materials hierarchical multiscale methods are developed where a macroscopic model exists for a properly selected set of macroscopic variables which need to be augmented with microscopic computations [2].

The so-called unit cell methods [21] are hierarchical multiscale methods in which the averaged microscopic stress-strain fields, computed on a representative unit cell of the microstructure subjected to a predefined loading path, are fitted to macroscopic closed form phenomenological constitutive equations in a format established *a priori.* For non-uniform microstructures, sufficiently large regions must be considered for analysis. Once the macroscopic response becomes nonlinear (geometric, material or both), it is extremely difficult to make a well-motivated assumption on a suitable macroscopic constitutive format.

The mathematical theory of asymptotic homogenization [22-24], which uses asymptotic expansions of field variables about macroscopic values has been developed as yet another hierarchical technique for analyzing multiscale response [11,25,27-30]. The asymptotic homogenization method provides overall effective properties as well as microscopic stress and strain values. However, the asymptotic homogenization method suffers from a major limitation stemming from its basic assumptions, *viz.* (a) uniformity of the macroscopic fields within each RVE and (b) local spatial periodicity of the RVE. Hence, this method breaks down in critical

regions of high gradients such as cracks, free edges, interfaces, neighborhoods of material discontinuities and in regions of evolving microstructural damage.

To extend the asymptotic homogenization method to nonperiodic problems, techniques such as the s-version of the finite element method [31,32], various multigrid-like bridging scale methods [33,34], an adaptive global-local method based on the Voronoi cell finite element method (VCFEM) [35], a homogenized Dirichlet projection method (HDPM) [36,37] and a generalized finite element method with "mesh-based handbook functions" [38] have been developed. The s-version of the finite element method is based on the principle of superimposed meshes [32] and requires cumbrous quadrature techniques. Unstructured multigrid-like methods require remeshing to capture evolving fine scale features. The VCFEM is an assumed stress hybrid method in which each heterogeneity is embedded in a Voronoi cell which is treated as a finite element. For ellipsoidal inclusions, in three-dimensions, stress functions which are elliptic integrals have to be approximately evaluated [35] and the method becomes intractable for complex 3D realistic microstructures. The homogenized Dirichlet projection method resolves the microstructural effects at different scales using an adaptive approach. An enormous number of local boundary value problems have to be solved to assemble the handbook function in [38] making the method rather impractical for general engineering applications.

To overcome problems associated with existing methods, a promising class of techniques is being developed to allow multiscale computations of problems involving arbitrary nonlinearites at the micro and macro-scales for general nonperiodic microstructures. These so-called "global-local" methods [10-12,15-17,20,26,35] do not lead to closed formed overall constitutive equations, but compute stress-strain relationship at every point of interest of the macro-component by detailed modeling of the microstructure attributed to this point. These techniques may be either explicit or implicit in nature. An explicit time marching algorithm is used in the explicit global-local methods to propagate the solution. In the implicit version, a Jacobian algorithm is necessary, which, of course, cannot be computed due to a lack of a closed formed constitutive expression at the macroscale.

For realistic problems with complex microstructures, not having to explicitly compute and store the Jacobian matrix at every Newton step is a major advantage in terms of storage requirements and computational cost compared to previous efforts based on homogenized material coefficients [12-14,19,35], condensation of the microscopic representative volume element (RVE) finite element stiffness matrix [15,20,39,40], and finite difference approximation of the material tangent matrix [16,18,40].

For the dynamical system an equation-free multiscale [41,42] has recently been proposed. Though the general philosophy of the equation-free approach is similar to that of the heterogeneous multiscale method [1], it differs in ways of dealing with the scale separation *i.e.* to use extrapolation in time and interpolation in space. If

micro-macro coupling is done within the framework of the Jacobian-free Newton Krylov method, the explicit formation of a Jacobian matrix can be avoided. Such Jacobian-free methods have been proposed recently to compute the macro-scale response of systems that allow clear scale separation by performing a sequence of micro-scale computations at each integration point of the discretized continuum [43]. However, the efficiency of this Jacobian-free multiscale approach depends on efficient preconditioning of the resulting Krylov subspace solver.

This chapter is organized as follows. The general global-local multiscale computational strategy is summarized in Section 2. In Sections 3 and 4 we outline the essence of explicit and implicit global-local multiscale methods. The issue of computational efficiency has been discussed in Section 5. Here we mainly focus on the coarse-grained parallelization techniques and matrix preconditioning strategy for the Jacobian-free multiscale method. In Section 6 we conclude with a discussion on existing techniques and an outlook for the future.

2 Global-local Multiscale Methods

A basic assumption of global-local methods is that clear scale separation exists. An example is a structural component model of a material that possesses an intricate spatial heterogeneity at a length scale small with respect to the structural dimensions but large with respect to atomic dimensions. Hence, the macro-scale may be modeled using continuum mechanics, while the micro-scale is modeled using an RVE, which may vary from one point of the macroscopic domain to the other. We review below the macroscopic and microscopic level continuum models along with the global-local solution strategy.

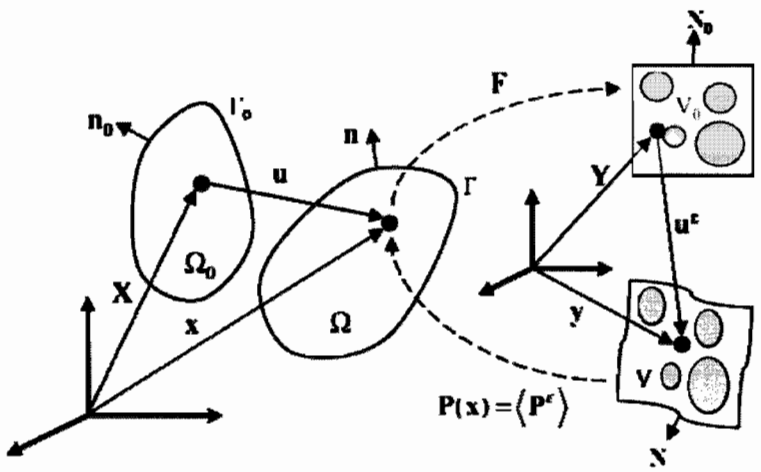

Figure 1: Macro-micro hierarchical multiscale computation strategy

2.1 Macroscale Problem

We consider a macroscopically homogeneous, but microscopically heterogeneous body which occupies $\Omega_0 \in \mathbb{R}^d$; $d \in \{1,2,3\}$ in the reference configuration that deforms to $\Omega \in \mathbb{R}^d$ following the map

$$\mathbf{x} = \varphi(\mathbf{X},t) \tag{1}$$

where **X** and **x** are points in the reference and deformed configurations, respectively, and 't' denotes time. For simplicity, we assume a total Lagrangian approach [44] in which the weak form of the governing equilibrium equations of elastodynamics at the macroscopic level may be stated as:
Find $\mathbf{u} = (\mathbf{x} - \mathbf{X}) \in H^1(\Omega_0 \times (0,T))$ *such that*

$$\int_{\Omega_0} \delta\mathbf{F}^T : \mathbf{P}\, d\Omega = \int_{\Omega_0} \delta\mathbf{u}^T \mathbf{b}^0\, d\Omega + \int_{\Gamma_t^0} \delta\mathbf{u}^T \bar{\mathbf{t}}^0\, d\Gamma \tag{2}$$

Satisfying;

$$\mathbf{u} = \bar{\mathbf{u}} \text{ on } \Gamma_u^0 \times (0,T) \tag{3}$$

$$\mathbf{u}(\mathbf{x}, t=0) = {}^0\mathbf{u} \text{ on } \Omega_0 \tag{4}$$

$$\dot{\mathbf{u}}(\mathbf{x}, t=0) = {}^0\dot{\mathbf{u}} \text{ on } \Omega_0 \tag{5}$$

where Ω_0 is an open bounded domain with boundary $\Gamma^0 = \Gamma_t^0 \cup \Gamma_u^0$; $\Gamma_t^0 \cap \Gamma_u^0 = 0$ (Figure 1) in the reference configuration; **F** is the deformation gradient tensor; **P** is the first Piola-Kirchhoff stress tensor; $\mathbf{b}^0$ is the body force per unit reference volume (including inertia forces); $\bar{\mathbf{t}}^0$ is the surface traction on the macroscopic boundary Γ_t^0 and H^1 is the first order Hilbert space. We will not define any constitutive equations to close this system.

2.2 Microscale Problem

Associated with each macro-scale point **X** is a mirco-scale representative volume element (RVE) which is assumed to deform from reference configuration $V_0 \in \mathbb{R}^d$ to $V \in \mathbb{R}^d$ (Figure 1) following the map

$$\mathbf{y} = \xi(\mathbf{Y},t) \tag{6}$$

where **Y** and **y** are points in the reference and deformed configurations of the RVE. The RVE is assumed to be free of body forces and the corresponding weak form is:
Find $\mathbf{u}^\varepsilon = (\mathbf{y} - \mathbf{Y}) \in H^1(V_0)$ *such that*

$$\int_{V_0} \delta\mathbf{F}^{\varepsilon T} : \mathbf{P}^\varepsilon dV_0 = 0 \tag{7}$$

where a suffix of 'e' denotes microscopic quantities. $\mathbf{F}^e$ and $\mathbf{P}^e$ are the microscopic deformation gradient tensor and first Piola-Kirchhoff stress tensor, respectively. The micro-scale system of equations is closed by known constitutive response of the constituents. Observe that there are no body forces acting on the RVE. Explicit constitutive equations are necessary for the micro-scale constituents to close the system of equations.

2.2.1 Choice of RVE

The RVE corresponding to a material point ($\mathbf{x}$) in the continuum is a material volume which is statistically representative of the infinitesimal material neighborhood of the material point. In this case, the size of the RVE is determined when the condition of statistical homogeneity is satisfied for all state variables [45]. Also, it should include only those dominant constituents that have a first order influence on the material properties of interest and that yield the simplest model. However, the choice of the RVE is non-trivial as discussed in detail in [46-48]. Here it is assumed that a choice has already been made and there are no body forces acting on the RVE.

2.2.2 RVE Boundary Conditions

The microscopic stress and strain fields may be obtained by solving the boundary value problems for the RVE with prescribed displacement/traction or periodic boundary conditions obtained from the macroscale problem, stated as:

$$\textit{Prescribed displacement: } \mathbf{y} = \mathbf{F}(\mathbf{x})\mathbf{Y} \quad \textit{for } \mathbf{Y} \in \partial V_0 \tag{8}$$

$$\textit{Prescribed traction: } \mathbf{t} = \mathbf{P}(\mathbf{x})^T \mathbf{N}_0(\mathbf{Y}) \quad \textit{for } \mathbf{Y} \in \partial V_0 \tag{9}$$

$$\textit{Periodic: } \mathbf{y}^+ - \mathbf{y}^- = \mathbf{F}\left(\mathbf{Y}^+ - \mathbf{Y}^-\right) \textit{ for } \mathbf{Y} \in \partial V_0 \tag{10}$$

where $\mathbf{F}$ and $\mathbf{P}(\mathbf{x})$ are the deformation gradient tensor and first Piola Kirchhoff stress corresponding to the point $\mathbf{x}$ in the macroscale to which the RVE is associated and $\mathbf{N_0}(\mathbf{Y})$ is the unit outward normal to the RVE boundary in the undeformed configuration at a point $\mathbf{Y}$. In the periodic boundary condition case the RVE boundary is split into two parts ∂V_0^+ and ∂V_0^- such that $\mathbf{N}_0^+ = -\mathbf{N}_0^-$.

In the next section we will show that corresponding to the prescribed displacement and periodic boundary conditions the volume averaged deformation gradient tensor within the RVE is $\mathbf{F}$, whereas, corresponding to the prescribed traction boundary condition, the volume averaged stress in the RVE is $\mathbf{P}(\mathbf{x})$.

In [49,50] it is observed that the periodic boundary conditions provide a better estimation of the overall properties than the prescribed displacement/traction boundary conditions. Contrary to the assumption of global periodicity, in [20] the periodic boundary condition implies a "locally periodic" microstructure in the

immediate vicinity of the individual macroscopic points. The microstructure may therefore have different morphologies at different macroscopic points.

2.3 Macro-Micro Coupling

The macroscopic computations at any point **x** provide the boundary conditions to the RVE associated with that point through the deformation gradient tensor (**F**) [10-14]. For the prescribed displacement boundary condition as in Equation (8), the volume average of the micro-scale deformation gradient tensor is:

$$\left\langle \mathbf{F}^{\varepsilon} \right\rangle = \frac{1}{|V_0|}\int_{V_0} \mathbf{F}^{\varepsilon} dV = \frac{1}{|V_0|}\int_{\partial V_0} \mathbf{y} \otimes \mathbf{N}\, dS = \frac{\mathbf{F}}{|V_0|}\int_{\partial V_0} \mathbf{Y} \otimes \mathbf{N}\, dS = \mathbf{F} \tag{11}$$

where **N** is the unit outward normal to the RVE in the reference configuration (Figure 1). The volume averaged microscopic stress

$$\left\langle \mathbf{P}^{\varepsilon} \right\rangle = \frac{1}{|V_0|}\int_{V_0} \mathbf{P}^{\varepsilon} dV_0 \tag{12}$$

is returned to the macro-scale as the stress corresponding to the point **x**, *i.e.*, **P**.

2.4 Computation of Effective Moduli: One-Dimensional Example

Consider a model 1D bar:

$$\frac{d}{dx}\left(E * \frac{du}{dx} \right) = 0\,;\ \forall x \in (0,1) \tag{13}$$

Satisfying Dirichlet boundary condition:

$$u(0) = 0; u(1) = \bar{u} \tag{14}$$

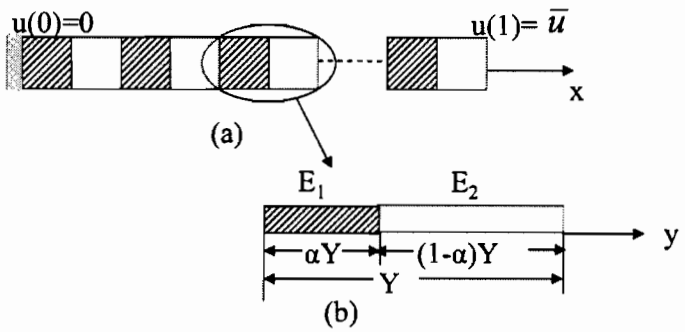

Figure 2: (a) Heterogeneous bar of unit length; (b) the RVE

2.4.1 Global-local Multiscale Approach

Assume the simple RVE of the following form with Dirichlet bc:

$$\frac{d}{dy}E(y)\frac{du}{dy}=0;\ \forall y\in(0,1) \tag{15}$$

$$u(y=0)=0;u(y=1)=u* \tag{16}$$

Integrate once:

$$E(y)\frac{du}{dy}=D\ \Rightarrow\frac{du}{dy}=\frac{D}{E(y)} \tag{17}$$

$$\Rightarrow\int_0^1\frac{du}{dy}dy=\int_0^1\frac{D}{E(y)}dy \tag{18}$$

$$\Rightarrow u^*-0=D\left(\frac{\alpha}{E_1}+\frac{1-\alpha}{E_2}\right) \tag{19}$$

$$\Rightarrow D=\frac{u^*}{\left(\frac{\alpha}{E_1}+\frac{1-\alpha}{E_2}\right)} \tag{20}$$

Hence, the average strain in the RVE

$$\langle\varepsilon\rangle=\int_0^1\frac{du}{dy}dy=\int_0^1\frac{D}{E(y)}dy=D\left(\frac{\alpha}{E_1}+\frac{1-\alpha}{E_2}\right)=u^* \tag{21}$$

The average stress in the RVE

$$\langle\sigma\rangle=\int_0^1E(y)\frac{du}{dy}dy=D=\frac{\langle\varepsilon\rangle}{\left(\frac{\alpha}{E_1}+\frac{1-\alpha}{E_2}\right)} \tag{22}$$

Since,

$$\sigma=E(y)\frac{du}{dy}=D \tag{23}$$

The effective modulus is therefore

$$E^*=\left(\frac{\alpha}{E_1}+\frac{1-\alpha}{E_2}\right)^{-1}\ \text{which relates}\ \langle\sigma\rangle=E^*\langle\varepsilon\rangle \tag{24}$$

2.4.2 Asymptotic Homogenization

If the displacement field $u(x)$ has periodicity Y, it can be approximated in terms of macroscopic and microscopic spatial coordinate x and $y = x / \varepsilon$, such that:

$$u(x, y(x)) = u(x, y) = u(x, y + kY); k = 1,2... \tag{25}$$

where $0<\varepsilon<<1$ denotes the size of the unit cell or period. Here we are assuming that E(x) is an oscillatory periodic coefficient. Now, consider the following asymptotic expansion of the displacement field $u(x,y)$:

$$u(x, y) = u_0(x, y) + \varepsilon u_1(x, y) + \varepsilon^2 u_1(x, y) + O(\varepsilon^3) \tag{26}$$

Substituting the asymptotic expansion of $u(x,y)$ into the above equilibrium equation yields equilibrium equations:

$$O(\varepsilon^{-2}): \frac{\partial}{\partial y}\left[E \frac{\partial u_0}{\partial y} \right] = 0 \tag{27}$$

The leading order equilibrium equation suggests that the leading order term in the asymptotic hierarchy is the function of macroscopic coordinate alone *i.e.* $u_0(x)$.

$$O(\varepsilon^{-1}): \frac{\partial}{\partial y} E(y)\left(\frac{\partial u_1}{\partial y} + \frac{\partial u_0}{\partial x} \right) = 0 \tag{28}$$

Integrate once:

$$E(y)\left(\frac{\partial u_1}{\partial y} + \frac{\partial u_0}{\partial x} \right) = c_1(x) \tag{29}$$

Integrate over RVE and by exploiting periodicity it gives:

$$c_1(x) = \frac{\partial u_0}{\partial x}\left(\frac{1}{Y} \int_Y \frac{1}{E(y)} dy \right)^{-1} \tag{30}$$

$$\Rightarrow \frac{\partial u_1}{\partial y} = \left[\frac{1}{E(y)}\left(\frac{1}{Y} \int_Y \frac{1}{E(y)} dy \right)^{-1} - 1 \right] \frac{\partial u_0}{\partial x} \tag{31}$$

$$O(\varepsilon^0): \frac{\partial}{\partial y}\left[E(y)\left(\frac{\partial u_2}{\partial y} + \frac{\partial u_1}{\partial x} \right) \right] + \frac{\partial}{\partial x}\left[E(y)\left(\frac{\partial u_0}{\partial x} + \frac{\partial u_1}{\partial y} \right) \right] = 0 \tag{32}$$

Integrating over RVE, dividing by Y and exploiting periodicity yields:

$$\Rightarrow \frac{\partial}{\partial x} c_1(x) = \frac{\partial}{\partial x}\left\{ \left(\frac{1}{Y} \int_Y \frac{1}{E(y)} dy \right)^{-1} \frac{\partial u_0}{\partial x} \right\} = 0 \tag{33}$$

Hence the homogenized material property is:

$$\Rightarrow E^* = \left(\frac{1}{Y} \int_Y \frac{1}{E(y)} dy \right)^{-1} = \left(\int_0^1 \frac{1}{E(y)} dy \right)^{-1} = \left(\frac{\alpha}{E_1} + \frac{1-\alpha}{E_2} \right)^{-1} \tag{34}$$

This is the same elastic constant as in case of global local multiscale computation in the previous section when periodic boundary conditions are applied.

3 Explicit Global-Local Multiscale Methods

To solve the weak form at the macro-scale (Equation (2)), we assume an approximation using finite elements

$$\mathbf{u}(\mathbf{X},t) \approx \mathbf{H}(\mathbf{X})\,\mathbf{U}(t) \tag{35}$$

where $\mathbf{H}(\mathbf{X})$ is the shape function matrix expressed in terms of the reference coordinates [44] and $\mathbf{U}(t)$ is the vector of nodal displacements. Hence, Equation (2) results in the discretized set of equations

$$\mathbf{M}\,\ddot{\mathbf{U}} = \mathbf{R} - \mathfrak{I} \tag{36}$$

where $\mathbf{M}$ is the mass matrix, $\mathbf{R}$ is the vector of externally applied nodal point loads

$$\mathbf{R} = \int_{\Omega_0} \mathbf{H}^T \tilde{\mathbf{b}}^0 d\Omega_0 + \int_{\Gamma_t^0} \mathbf{H}^T \bar{\mathbf{t}}^0 d\Gamma_t^0 \tag{37}$$

where $\tilde{\mathbf{b}}^0$ is the body force per unit reference volume excluding inertia forces. In Equation (36) $\mathfrak{I}$ is the vector of nodal point forces corresponding to element stresses

$$\mathfrak{I} = \int_{\Omega_0} \mathbf{B}^T : \mathbf{P}\, d\Omega_0 \tag{38}$$

where,

$$\mathbf{B}(\mathbf{X}) = \nabla_{\mathbf{X}} \mathbf{H}(\mathbf{X}) \tag{39}$$

The solution of the nodal point displacement at time '$t+\Delta t$' is obtained using an explicit time integration scheme, such as the central difference method [44], for the acceleration ($\ddot{\mathbf{U}}$) in Equation (36), *i.e.*,

$${}^{t}\ddot{\mathbf{U}} = \frac{1}{\Delta t^2}\left({}^{t-\Delta t}\mathbf{U} - 2\,{}^{t}\mathbf{U} + {}^{t+\Delta t}\mathbf{U} \right) \tag{40}$$

If a diagonal mass matrix $\mathbf{M} = diag(m_{ii})$ is chosen, the solution corresponds to a forward marching in time, where each component of the displacement at time ${}^{t+\Delta t}U_i$ may be directly computed in a matrix-free manner as

$${}^{t+\Delta t}U_i = 2\,{}^{t}U_i - {}^{t-\Delta t}U_i + \frac{\Delta t^2}{m_{ii}}\left({}^{t}R_i - {}^{t}\mathfrak{I}_i \right) \quad i = 1,2,\ldots, NDOF \tag{41}$$

where '*NDOF*' is the total number of degrees of freedom of the macro-scale model.

In the finite element method, the right hand sides of Equations (37) and (38) are computed using Gauss integration, *e.g.*,

$$^{t}\mathfrak{I} = \int_{\Omega_0} \mathbf{B}^T : {}^{t}\mathbf{P} d\Omega_0 \approx \sum_{IP=1}^{NGAUSS} W_{IP} \left(\mathbf{B}^T : {}^{t}\mathbf{P} \right)_{\mathbf{X}=\mathbf{X}_{IP}} \tag{42}$$

where *NGAUSS* is the total number of Gauss quadrature points in the finite element model, W_{IP} and $\mathbf{X}_{IP}$ are the integration weights and points, respectively. At each macroscopic Gauss point, the deformation gradient tensor is computed and is used to apply boundary conditions to the RVE as in Equation (8). The resulting stress is volume-averaged on the RVE to compute the stress at the macro-scale using Equation (12). The steps involved in the sequential explicit global-local model are summarized in Algorithm-1.

Algorithm-1: Explicit global-local multiscale model

1 *for* each time step $t \rightarrow t + \Delta t$
2 *for* each **macro-scale** Gauss point
3 Compute $^{t}\mathbf{F} = \mathbf{I} + \mathbf{B}\,{}^{t}\mathbf{U}$
4 Solve the **micro-scale** problem with bc $\mathbf{y} = {}^{t}\mathbf{F}\mathbf{Y}$ for $\mathbf{P}^{\varepsilon}$
5 Compute $^{t}\mathbf{P} = \left\langle \mathbf{P}^{\varepsilon} \right\rangle$
6 *end for*
7 Compute $^{t}\mathfrak{I}$, $^{t}\mathbf{R}$
8 Compute the displacement at time $t + \Delta t$

$$^{t+\Delta t}\mathbf{U} = 2\,{}^{t}\mathbf{U} - {}^{t-\Delta t}\mathbf{U} + \frac{\Delta t^2}{m_{ii}} \left({}^{t}\mathbf{R} - {}^{t}\mathfrak{I} \right)$$

9 *end for*

4 Implicit Global-Local Multiscale Methods

In this section we briefly present the essence of an implicit multiscale method for the solution of BVP problems in computational mechanics. Using the following finite element discretization of the displacement field at the macroscale

$$\mathbf{u}(\mathbf{X}) \approx \mathbf{H}(\mathbf{X})\mathbf{U} \tag{43}$$

where $\mathbf{H}(\mathbf{X})$ is the matrix of shape functions matrix expressed in terms of the reference coordinates [44] and $\mathbf{U}$ is the vector of nodal displacements, the discretized form of Equation (2), after incorporating the Direchlet boundary conditions, is

Find $\mathbf{U} \in \mathbb{R}^n$ *such that*

$$\Psi(\mathbf{U}) = \mathbf{f} - \Phi(\mathbf{U}) = \mathbf{0} \tag{44}$$

where 'n' is the number of degrees of freedom of the macroscale problem, $\mathbf{f}$ is the vector of externally applied nodal point loads

$$\mathbf{f} = \int_{\Omega_0} \mathbf{H}^T \mathbf{b}^0 d\Omega_0 + \int_{\Gamma_t^0} \mathbf{H}^T \bar{\mathbf{t}}^0 d\Gamma_t^0 \tag{45}$$

and $\Phi(\mathbf{U})$ is the vector of internal forces corresponding to element stresses

$$\Phi(\mathbf{U}) = \int_{\Omega_0} \mathbf{B}^T : \mathbf{P} d\Omega_0 \tag{46}$$

where $\mathbf{B}(\mathbf{X}) = \nabla_{\mathbf{X}} \mathbf{H}(\mathbf{X})$ is the strain-displacement matrix.

The solution of Equation (44) using Newton-Raphson iterations involves finding the Newton directions $\delta \mathbf{U}^k$ at every Newton step by solving the following equation

$$\mathbf{J}(\mathbf{U}^k) \delta \mathbf{U}^k = -\Psi(\mathbf{U}^k) \tag{47}$$

In this equation, $\mathbf{J}(\mathbf{U}^k)$ is the Jacobian

$$\mathbf{J}(\mathbf{U}^k) = \frac{\partial \Psi(\mathbf{U}^k)}{\partial \mathbf{U}^k} = -\frac{\partial \Phi(\mathbf{U}^k)}{\partial \mathbf{U}^k} = -\int_{\Omega_0} \mathbf{B}^T : \frac{\partial \mathbf{P}^k}{\partial \mathbf{E}^k} : \frac{\partial \mathbf{E}^k}{\partial \mathbf{U}^k} d\Omega_0 \tag{48}$$

where $\mathbf{E}^k = \frac{1}{2}(\mathbf{F}^{k^T} \mathbf{F}^k - \mathbf{I})$ is the Green-Lagrange strain.

In a multiscale problem, the constitutive equation at the macro-scale is unknown and therefore the Jacobian cannot be computed in closed-form. In Section 4.1 we review some of the existing approaches of Jacobian approximation, whereas, in Section 4.2 will present the essence of the Jacobian-free multi-scale model that does not require an explicit Jacobian formation to solve the resulting macroscopic problem.

4.1 Jacobian Computation Strategies

In literature various methods have been proposed to deal with the computation of the Jacobian at the macroscopic scale. In the following sections we will discuss four classes of methods which are found in literature.

4.1.1 Techniques Based on Condensation

One class of methods for approximately computing the global Jacobian matrix is based on condensation of the microscale finite element stiffness matrix or material tangent modulus [15,20,26,39,40]. For example in [20] at each of the macroscopic integration points the consistent stiffness matrix is derived by reducing the total RVE stiffness matrix to the relation between the forces $\mathbf{f}_p$ acting on the retained vertices of the RVE and the displacements $\mathbf{u}_p$ of these vertices, where, subscript 'p' stands for prescribed quantity. For the first-order gradient based approach, when the

RVE is deformed under prescribed boundary displacement, Equation (??), this relation is

$$\mathbf{K}_M \delta \mathbf{u}_p = \delta \mathbf{f}_p \tag{49}$$

where $\mathbf{K}_M$ is the condensed RVE stiffness matrix. Equation (49) is used to derive the consistent tangent at the macroscopic integration point. From Equation (12)

$$\begin{aligned}\left\langle \mathbf{P}^{\varepsilon} \right\rangle &= \frac{1}{|V_0|}\int_{V_0} \mathbf{P}^{\varepsilon} dV_0 \\ &= \frac{1}{|V_0|}\int_{V_0}\left[\nabla_{\mathbf{Y}}\cdot\left(\mathbf{P}^{\varepsilon}\right)^T \otimes \mathbf{Y} + \left(\mathbf{P}^{\varepsilon}\right)^T \nabla_{\mathbf{Y}}\mathbf{Y}\right] dV_0 \\ &= \frac{1}{|V_0|}\int_{\partial V_0}\left(\mathbf{P}^{\varepsilon}\right)^T \mathbf{N}\otimes\mathbf{Y} dS = \frac{1}{|V_0|}\int_{\partial V_0}\mathbf{f}_p \otimes \mathbf{Y} dS \quad \because \nabla_{\mathbf{Y}}\cdot\left(\mathbf{P}^{\varepsilon}\right)^T = \mathbf{0} \text{ and } \nabla_{\mathbf{Y}}\mathbf{Y} = \mathbf{I}\end{aligned} \tag{50}$$

For the case of prescribed displacement boundary conditions and using Equation (49) the variation of $\left\langle \mathbf{P}^{\varepsilon} \right\rangle$ then leads to:

$$\begin{aligned}\delta\left\langle \mathbf{P}^{\varepsilon} \right\rangle &= \frac{1}{|V_0|}\int_{\partial V_0} \delta\mathbf{f}_p \otimes \mathbf{Y} dS \\ &= \frac{1}{|V_0|}\int_{\partial V_0} \mathbf{K}_M \delta\mathbf{u}_p \otimes \mathbf{Y} dS \\ &= \frac{1}{|V_0|}\int_{\partial V_0} \mathbf{K}_M \delta\mathbf{F}\left(\mathbf{Y}\otimes\mathbf{Y}\right) dS \quad \because \delta\mathbf{u}_p = \delta\mathbf{F}\mathbf{Y} \\ &= \left[\frac{1}{|V_0|}\int_{\partial V_0} \mathbf{Y}\otimes\mathbf{K}_M\otimes\mathbf{Y} dS\right]^{LC} : \delta\mathbf{F}^T\end{aligned} \tag{51}$$

where the superscript *LC* stands for 'left conjugate'. From Equation (51) the consistent tangent **L** is identified as:

$$\mathbf{L} = \left[\frac{1}{|V_0|}\int_{\partial V_0} \mathbf{Y}\otimes\mathbf{K}_M\otimes\mathbf{Y}\, dS\right]^{LC} \tag{52}$$

Higher order gradient-based approach

A higher order gradient-based global-local multiscale method has been outlined in [51] and motivated by modeling the microstructural size effect. This uses a gradient second-order equilibrium problem at the macroscale, while the microscopic equilibrium problem follows classical continuum theory. In this approach, the RVE kinematic boundary condition is determined by the combination of macroscopic deformation gradient tensor **F** and its gradient $\nabla_X \mathbf{F}$. The macroscopic first Piola-Kirchhoff stress tensor **P** and the higher-order stress tensor **Q** is then derived using a modified Hill-Mandel condition [51]. The latter can be interpreted as the first

moment, with respect to the RVE center, of the microscopic first Piola-Kirchhoff stress tensor $\mathbf{P}^{\varepsilon}$ over the initial RVE volume V_0

$$\mathbf{Q} = \frac{1}{2|V_0|}\int_{V_0}\left(\mathbf{P}^{\varepsilon}\right)^{T}\otimes\mathbf{Y} + \mathbf{Y}\otimes\mathbf{P}^{\varepsilon}\,dV_0 \tag{53}$$

The macroscopic consistent tangent derivation is based on similar ideas outlined for the first-order gradient-based approach.

4.1.2 Techniques Based on Asymptotic Homogenization

For the small-deformation and locally periodic microstructure, the classical asymptotic homogenization based global-local approach is used to obtain the homogenized material coefficients to form the macroscopic consistent tangent matrix [12-14,19,35]. Here, it is assumed that the **Y**-periodic microscopic displacement is linear with respect to the macroscopic strains, *i.e.*

$$\mathbf{u}(\mathbf{y}=\mathbf{x}/\varepsilon,\mathbf{x}) = \chi^{kh}(\mathbf{y})\frac{\partial u_k^0(\mathbf{x})}{\partial x_h} + \mathbf{c}(\mathbf{x}) \tag{54}$$

where $\chi^{kh}(\mathbf{y})$ is a **Y**-periodic function representing characteristic modes of the microstructure, $\mathbf{c}(\mathbf{x})$ is a constant independent of $\mathbf{y}$ and 'ε' is the perturbation parameter. Under these assumptions the homogenized tangent modulus is

$$\mathbf{L} = \frac{1}{|V|}\int_{V}\mathbf{L}^{\varepsilon} : \left({}^{4}\mathbf{I} + \nabla_y\chi\right)dV \tag{55}$$

where ${}^{4}\mathbf{I}$ is the fourth-order identity tensor.

4.1.3 Techniques Based on Finite Difference Approximation

The consistent tangent moduli can be computed numerically by using forward difference approximation of the material tangent modulus [16,18,40] as:

$$\mathbf{L}^{ijkl} \equiv \frac{\partial\mathbf{P}^{ij}}{\partial\mathbf{F}_{kl}} \approx \frac{1}{\eta}\left[\mathbf{P}^{ij}(\mathbf{F}_{kl}+\eta\mathbf{e}_k\otimes\mathbf{e}_l) - \mathbf{P}^{ij}(\mathbf{F}_{kl})\right] \tag{56}$$

where the perturbation parameter η is used to compute the perturbed macroscopic deformation gradient. The indices (*ij*) and (*kl*) correspond to the rows and columns of the corresponding **L** matrix in Voigt notation. The quality of approximation in Equation (56) largely depends on the choice of the perturbation parameter η. Possible choices of η and the corresponding error estimate are discussed in [52].

4.1.4 Techniques Based on Newton-Krylov Approximation

In the Jacobian-free multiscale method [42,43], Equation (47) is solved iteratively to approximately find the Newton directions

$$\delta \mathbf{U}_m^k = \delta \mathbf{U}_0^k + \mathbf{V}_m^k \mathbf{z}_m^k \tag{57}$$

where 'm' denotes the Krylov iteration step, $\delta \mathbf{U}_0^k$ is the initial guess (usually assumed **0**), and $\mathbf{V}_m^k \in \mathbb{R}^{n \times m}$ is the 'Krylov matrix' whose columns are the orthonormalized Krylov vectors ($\mathbf{v}_j^k$), *i.e.*,

$$\mathbf{V}_m^k = \left[\mathbf{v}_j^k \right]_{1 \le j \le m} \text{ with } \left(\mathbf{v}_i^k \right)^T \mathbf{v}_j^k = \delta_{ij} \tag{58}$$

If the generalized minimal residual (GMRES) algorithm is used [53], then in Equation (57) $\mathbf{z}_m^k$ is computed by solving the least squares problem

$$\min_{\mathbf{z}_m^k \in R^m} \left\| \beta \mathbf{e}_1 - \bar{\mathbf{H}}_m^k \mathbf{z}_m^k \right\| \tag{59}$$

where $\bar{\mathbf{H}}_m^k \in \mathbb{R}^{(m+1) \times m}$ is a rectangular upper Hessenberg matrix whose entries are

$$h_{i,j}^k = \begin{cases} \left(\mathbf{v}_i^k \right)^T \mathbf{J}^k \mathbf{v}_j^k & i \le j+1 \\ 0 & i > j+1 \end{cases} \tag{60}$$

with $\mathbf{J}^k \equiv \mathbf{J}(\mathbf{U}^k)$. $\mathbf{e}_1$ is the unit vector with '1' as its first entry and $\beta = \|\mathbf{r}_0\|$ where

$$\mathbf{r}_0 = \mathbf{J}(\mathbf{U}^k) \delta \mathbf{U}_0^k + \Psi(\mathbf{U}^k) \tag{61}$$

is the initial residual.

At the heart of the GMRES algorithm is the Arnoldi factorization

$$\mathbf{J}^k \mathbf{V}_m^k = \mathbf{V}_m^k \mathbf{H}_m^k + h_{m+1,m}^k \mathbf{v}_{m+1}^k \mathbf{e}_m^T \tag{62}$$

which allows the computation of the component $h_{m+1,m}^k$ of the upper Hessenberg matrix and the $(m+1)^{\text{th}}$ Arnoldi vector $\mathbf{v}_{m+1}^k$ by performing matrix-vector products involving the Jacobian matrix and the previous Arnoldi vector according to the following relationships

$$h_{m+1,m}^k = \left\| \mathbf{J}^k \mathbf{v}_m - \sum_{k=1}^{m} h_{km} \mathbf{v}_k \right\| \tag{63}$$

$$\mathbf{v}_{m+1}^k = \frac{\mathbf{J}^k \mathbf{v}_m - \sum_{k=1}^{m} h_{km} \mathbf{v}_k}{h_{m+1,m}} \tag{64}$$

Since the Jacobian matrix ($\mathbf{J}^k$) is not explicitly computed, the matrix-vector product in Equations (63) and (64) is approximated using the following finite difference approximation [54]

$$\mathbf{J}^k\mathbf{v}_m = \frac{\partial \Psi(\mathbf{U}^k)}{\partial \mathbf{U}^k}\mathbf{v}_m = -\frac{\partial \Phi(\mathbf{U}^k)}{\partial \mathbf{U}^k}\mathbf{v}_m \approx -\frac{\Phi(\mathbf{U}^k + \theta\mathbf{v}_m) - \Phi(\mathbf{U}^k)}{\theta} \tag{65}$$

where θ is a scalar perturbation parameter. It has been shown in [52,54] that an optimal choice of θ is

$$\theta = \frac{\sqrt{\varepsilon}}{\|\mathbf{v}_m\|_2}\max\left\{\left|\left(\mathbf{U}^k\right)^T\mathbf{v}_m\right|, \left(typ\mathbf{U}^k\right)^T|\mathbf{v}_m|\right\} sign\left(\left(\mathbf{U}^k\right)^T\mathbf{v}_m\right) \tag{66}$$

where $typ\mathbf{U}^k$ is a user-supplied "typical size" or "scaling" of components of $\mathbf{U}^k$, $|\mathbf{v}_m| = \left[|v_{m_1}|, \ldots, |v_{m_n}|\right]^T$ and e is the machine epsilon. $\Phi(\mathbf{U}^k + \theta\mathbf{v}_m)$ in Equation (65) is computed by applying suitable perturbations to the micro-scale RVE.

4.1.4 Comparative Analysis

If we compare the consistent tangent modulus computation using an asymptotic homogenization based approach with the rest of the approaches outlined above, it is evident that the former is limited to small deformation problems with locally periodic microstructures. The condensation-based approach is computationally efficient, however, its success relies on the choice of the prescribed boundary nodes, which may not be a trivial task in three-dimensional analysis. The numerical computation of the consistent tangent moduli using the forward difference approximation is more accurate, however, it may not be as computationally efficient as the condensation-based approach. The Newton-Krylov based implicit approximation scheme is efficient for realistic problems with complex microstructures. Not having explicitly to compute and store the consistent tangent moduli is a major advantage of this method in terms of storage requirements and computational cost compared to the other methods outlined above.

5 Computational Efficiency

The existing global-local multiscale computational methods, *e.g.* using finite element discretization at both the macro- and micro-scales, are intensive both in terms of computational time and memory requirements. For these methods to be widely used in the solution of practical problems it is important to ensure both the efficiency and reliability of these methods. While there has been excellent progress in the development of multiscale methods, the issue of efficiency has not received sufficient attention. In Section 5.1 we review an efficient coarse grain parallel scheme for global-local multiscale methods [55], while, in Section 5.2 we present a block preconditioning strategy that accelerates the convergence of Jacobian-free multiscale methods.

5.1 Coarse-Grained Parallel Algorithms

The coupled macro-micro computation in the global-local multiscale problem poses severe computational bottleneck. Traditionally, this issue is addressed by adopting it to the domain decomposition based parallel algorithm, which is originally designed for the finite element computations [18, 56, 57]. In [58, 59], a multi-level parallel algorithm is developed for an adaptive multi-scale finite element model. Departing from the traditional approach, in [57], two stages of micro-scale computations for the tangential homogenization and the microscopic self-equilibrium are proposed to distribute on the set of a PC-cluster while the macro-scale computation is performed on a single processor.

The major limitation of the domain-decomposition based approach is the sequential computation of the microscale problem on the processor assigned to a particular sub-domain. It also suffers from an extensive communication overhead across the sub-domain, which inturn limits the maximum degree of concurrency that can be achieved. To overcome these issues, in [57], the macro-scale problem is computed sequentially on a single processor, whereas the micro-scale problem is distributed among the rest of the available processors. This approach eliminates some of the shortcomings of a domain-decomposition based approach at the cost of extensive communication within a larger group of micro-layer processors and their idling due to sequential computation of the macro-scale problem.

The matrix-free global-local approach requires computation of the vector of nodal point forces corresponding to element stresses that may be performed using the volume averaged RVE stresses. This eliminates the need for specialized graph partition techniques that inturn minimize the communication overhead. The matrix-free architecture is particularly suitable for mapping two scales of a global-local multiscale model on a massively parallel platform (MPP). This is because of its innate requirement to compute the micro-scale problems on the micro-layer processors in a coarse-grained sense at optimal cost to macro-micro communication.

We have developed algorithms for parallelizing both implicit and explicit [55] matrix-free global-local multiscale methods. Taking advantage of the hierarchical nature of the macro-micro computation, we distribute the groups of macro-scale integration points to one layer of processors. In this layer processors communicate locally with a group of processors that are assigned for the micro-scale computations. The macro-scale problem is decomposed using logical hierarchical topology developed in ref. [55]. This type of decomposition ensures equal computational load sharing among a macroscopic group of processors, each of which overlaps and hence communicates with a local group of processors in the microscopic layer without any specific need for an inter-group communicator.

5.2 Preconditioning Strategy for Jacobian-Free Multiscale

In implicit global-local methods which use iterative solvers [42,43,60], considerable advantage may be gained by using a preconditioner. In [42], a physics-based left

preconditioner is developed to accelerate the GMRES iterations, which is based on a central finite difference time-stepper approximately to represent the coarse scale model. In [60], a two-level coarse grid correction preconditioner is used to correct the non-converging and slowly converging low-frequency eigenmodes. However, these techniques may still require Jacobian approximation at some level for preconditioning the Krylov subspace solver.

For Jacobian-free multiscale methods, it is desirable to develop a preconditioner which is efficient, yet general enough to be independent of the physics of the problem being solved. Such a preconditioner should accelerate the convergence of the Newton-Krylov process without incurring an additional computational overhead at the micro-scale, *i.e.*, without explicitly computing the Jacobian at any of the Newton steps. We have developed a block right preconditioner [43] that effectively deflates the spectrum of the Jacobian matrix corresponding to the current Newton step by using information from the Krylov subspaces spanned by a few of the Arnoldi vectors corresponding to the previous Newton steps and the representation of the Jacobians on those bases. In principle, this is based on the strategy presented in [61] for a restarted GMRES. Notice that this method does not involve explicit Jacobian computation at any Newton step. This preconditioning strategy is powerful as each block in the preconditioner results in an eigenvalue of the preconditioned Jacobian matrix with multiplicity, which is at least equal to the dimension of the respective right invariant subspace. However, the effectiveness of the preconditioner depends on how close the respective blocks in the preconditioner estimates the eigenvalues of the current Jacobian matrix. We will briefly describe this preconditioner in the following paragraphs for a linear system

$$\mathbf{A}\mathbf{x} = \mathbf{b} \tag{67}$$

which is solved using GMRES. At the m^{th} step of the Arnoldi process, the matrix $\mathbf{A}$ permits the factorization [53]

$$\mathbf{V}_{m+1}{}^{T}\mathbf{A}\mathbf{V}_{m} = \bar{\mathbf{H}}_{m} \tag{68}$$

where $\mathbf{V}_{m+1} \in \mathbb{R}^{n\times(m+1)}$ and $\mathbf{V}_{m} \in \mathbb{R}^{n\times m}$ are Krylov matrices with orthonormal columns and $\bar{\mathbf{H}}_{m} \in \mathbb{R}^{(m+1)\times m}$ is an upper Hessenberg matrix which permits the following QR-factorization

$$\bar{\mathbf{H}}_{m} = \mathbf{Q}_{m}\mathbf{R}_{m} = \mathbf{Q}_{m+1}\bar{\mathbf{R}}_{m} \tag{69}$$

where $\mathbf{R}_{m} \in \mathbb{R}^{m\times m}$ and $\mathbf{Q}_{m} \in \mathbb{R}^{(m+1)\times m}$ is proper orthogonal. In Equation (69) $\bar{\mathbf{R}}_{m} = \left(\mathbf{R}_{m};\mathbf{0}\right)$ is obtained by inflating $\bar{\mathbf{R}}_{m}$ with an extra row of zeros and $\mathbf{Q}_{m+1} \in \mathbb{R}^{(m+1)\times(m+1)}$.

The basic idea in preconditioning is to solve the preconditioned set

$$\mathbf{A}\mathbf{M}^{-1}\mathbf{y} = \mathbf{b} \tag{70}$$

$$\mathbf{Mx} = \mathbf{y} \tag{71}$$

instead of the original one in Equation (67). For the $(k+1)^{th}$ Newton step, the form of the right preconditioner is

$$\left(\mathbf{M}^{k+1}\right)^{-1} = \mathbf{I}_n + \sum_{j=0}^{k} \mathbf{V}^j_{m_j+1} \left\{ \left(\alpha_j \left(\mathbf{R}^j_{m_j}\right)^{-1} \left(\mathbf{Q}^j_{m_j}\right)^T ; \left(\mathbf{Q}^j_{m_j+1} \mathbf{e}_{m_j+1}\right)^T \right) - \mathbf{I}_{m_j+1} \right\} \left(\mathbf{V}^j_{m_j+1}\right)^T \tag{72}$$

which uses information not just from step 'k', but from all previous Newton steps. In this equation, 'm_j' is the number of GMRES iterations for convergence in Newton step 'j', $\mathbf{V}^j_{m_j+1}$ is the Krylov matrix, $\mathbf{R}^j_{m_j}$ and $\mathbf{Q}^j_{m_j+1}$ are the QR factors of the corresponding upper Hessenberg matrix $\bar{\mathbf{H}}^j_{m_j} \in \mathbb{R}^{(m_j+1)\times m_j}$, $\alpha_j \in \mathbb{R}, \alpha_j \neq 0$, and $\mathbf{I}_{m_j} \in \mathbb{R}^{n\times m_j}$ is an identity matrix. The action of the block preconditioner in Equation (72) increases the multiplicity of '$k+1$' eigenvalues of the preconditioned Jacobian matrix at Newton step '$k+1$' by m_0, m_1, ..., m_k, respectively.

6 Concluding remarks

The ability of global-local multiscale methods to model arbitrary nonlinearities at the microscale without making *a priori* assumptions regarding local periodicity makes them powerful techniques for the solution of a large class of problems in science and engineering. Their applicability, however, is limited by the computational cost as well as memory requirements. For these methods to be applied to realistic problems, it is therefore important to ensure both efficiency and reliability. Advances in parallel computational technology, efficient preconditioning strategies and other acceleration techniques must be pursued to ensure efficiency. Multiscale error analysis, as well as studies related to numerical stability are also necessary to lay the foundations of reliable global local multiscale technology.

Acknowledgements

The authors gratefully acknowledge the support of this work through the Office of Naval Research (ONR), USA grants N000140510686 and N000140810462.

References

[1] E. Weinan, B. Engquist, X. Li, W. Ren, E. Vanden-Eijnden, "The heterogeneous multiscale method: A review", Communications in Computational Physics, 6, 367–450, 2007.

[2] S. Yip, "Handbook of materials modeling", XXIX ed. Springer, Berlin, 2005.

[3] S. Kolhoff, P. Gumbsch, H.F. Fishmeister, "Crack propagation in BCC crystals studied with a combined finite-element and atomistic model", Philosophical Magazine A, 64, 851–878, 1991.

[4] M. Mullins, M.A. Dokainish, "Simulation of the (001) plane crack in alpha-iron employing a new boundary scheme", Philosophical Magazine A, 46, 771–787, 1982.

[5] E.B. Tadmor, N. Ortiz, R. Phillips, "Quasicontinuum analysis of defects in solids", Philosophical Magazine A, 73, 1529–1563, 1996.

[6] F.F Abraham, N. Bernstein, J.Q. Broughton, D. Hess, "Dynamic fracture of silicon: concurrent simulation of quantum electrons, classical atoms, and the continuum solid", Materials Research Society Bulletin, 25, 27–32, 2000.

[7] R. Miller, V. Shenoy, M. Ortiz, E. Tadmor, R. Phillips, "Quasicontinuum models of fracture and plasticity", Engineering Fracture Mechanics, 61, 427–444, 1998.

[8] G.J. Wagner, W.K. Liu, "Coupling of atomistic and continuum simulations using a bridging scale decomposition", Journal of Computational Physics, 190, 249–274, 2003.

[9] S.P. Xiao, T. Belytschko, "A bridging domain method for coupling continua with molecular dynamics", Computer Methods in Applied Mechanics and Engineering, 193, 1645–1669, 2004.

[10] P.M. Suquet, "Local and global aspects in the mathematical theory of plasticity", in A. Sawczuk, G. Bianchi, (Editors), "Plasticity Today: Modelling, Methods and Applications", Elsevier Applied Science Publishers: London, 279–310, 1985.

[11] J.M. Guedes, N. Kikuchi, "Preprocessing and postprocessing for materials based on the homogenization method with adaptive finite element methods", Computer Methods in Applied Mechanics and Engineering, 83, 143–198, 1990.

[12] K. Terada, N. Kikuchi, "Nonlinear homogenization method for practical applications", In S. Ghosh, M. Ostoja-Starzewski, (Editors), "Computational Methods in Micromechanics", AMD-vol. 212/MD-vol. 62, ASME: New York, 1–16, 1995.

[13] S. Ghosh, K. Lee, S. Moorthy, "Multiple scale analysis of heterogeneous elastic structures using homogenization theory and Voronoi cell finite element method", International Journal of Solids and Structures, 32, 27–62, 1995.

[14] S. Ghosh, K. Lee, S. Moorthy, "Two scale analysis of heterogeneous elastic–plastic materials with asymptotic homogenisation and Voronoi cell finite element model", Computer Methods in Applied Mechanics and Engineering, 132, 63–116, 1996.

[15] R.J.M. Smit, W.A.M. Brekelmans, H.E.H. Meijer, "Prediction of the mechanical behaviour of non-linear heterogeneous systems by multi-level finite element modeling", Computer Methods in Applied Mechanics and Engineering, 155, 181–192, 1998.

[16] C. Miehe, J. Schroder, J. Schotte, "Computational homogenization analysis in finite plasticity. Simulation of texture development in polycrystalline

materials", Computer Methods in Applied Mechanics and Engineering, 171, 387–418, 1999.

[17] J.C. Michel, H. Moulinec, P. Suquet, "Effective properties of composite materials with periodic microstructure: a computational approach", Computer Methods in Applied Mechanics and Engineering, 172, 109 –143, 1999.

[18] F. Feyel, J.L. Chaboche, "FE2 multiscale approach for modelling the elastoviscoplastic behaviour of long fibre SiC/Ti composite materials", Computer Methods in Applied Mechanics and Engineering, 183, 309–330, 2000.

[19] K. Terada, N. Kikuchi, "A class of general algorithms for multi-scale analysis of heterogeneous media", Computer Methods in Applied Mechanics and Engineering, 190, 5427– 5464, 2001.

[20] V. Kouznetsova, W.A.M. Brekelmans, F.P.T Baaijens, "An approach to micro–macro modelling of heterogeneous materials", Computational Mechanics, 27, 37– 48, 2001.

[21] T. Zohdi, P. Wriggers, "Introduction to computational micromechanics", Lecture notes in applied Computational Mechanics, 20, Springer, 2004.

[22] N. Bakhalov, G. Panasenko, "Homogenisation: Averaging process in periodic media", Kluwer Academic Publishers, Dordrecht, The Neatherlands, 1989.

[23] A. Bensoussan, J.L. Lions, G. Papanicolaou, "Asymptotic analysis for periodic structures", North-Holland, Amsterdam, 1978.

[24] E. Sanchez-Palencia, A. Zaoui, "Homogenization techniques for composite media", Springer-Verlag, 1985.

[25] A. Tolenado, H. Murakami, "A high-order mixture model for periodic particulate composites", International Journal of Solids and Structures, 23, 989-1002, 1987.

[26] C. Miehe, A. Koch, "Computational micro-to-macro transition of discretized microstructures undergoing small strain", Computer Archives of Applied Mechanics, 72, 300-317, 2002.

[27] S.J. Hollister, D.P. Fyhrie, K.J. Jepsen, S.A. Goldstein, "Analysis of trabecular bone micro-mechanics using homogenization theory with comparison to experimental results", Journal of Biomechanics, 22(10), 1025, 1989.

[28] S.J. Hollister, D.P. Fyhrie, K.J. Jepsen, S.A. Goldstein, "Application of homogenization theory to the study of trabecular bone mechanics", Journal of Biomechanics, 24(9), 825-839, 1991.

[29] S.J. Hollister, N. Kikuchi, "A comparison of homogenization and standard mechanics analyses for periodic porous composites", Computational Mechanics, 10, 73-95, 1992.

[30] J. Fish, Q. Yu, K. Shek, "Computational damage mechanics for composite materials based on mathematical homogenization", International Journal for Numerical Methods in Engineering, 45, 1657-1679, 1999.

[31] J. Fish, "The s-version of the finite element method", Computers and Structures, 43(3), 539-547, 1992.

[32] J. Fish, A. Wagiman, "Multiscale finite element method for heterogeneous medium", Computational Mechanics, 12, 1-17, 1993.

[33] J. Fish, V. Belsky, "Multigrid method for periodic heterogeneous medium. Part I: Convergence studies for one-dimensional case", Computer Methods in Applied Mechanics and Engineering, 126, 1-16, 1995.
[34] J. Fish, V. Belsky, "Multigrid method for periodic heterogeneous medium. Part II: Multiscale modeling and quality control in multidimensional case", Computer Methods in Applied Mechanics and Engineering, 126, 1-16, 1995.
[35] S. Ghosh, K. Lee, P. Raghavan, "A multilevel computational model for multiscale damage analysis in composite and porous materials", International Journal of Solids and Structures, 38, 2335-2385, 2001.
[36] J.T. Oden, T.I. Zohdi, "Analysis and adaptive modeling of highly heterogeneous elastic structures", Computer Methods in Applied Mechanics and Engineering, 148, 367-391, 1997.
[37] J.T. Oden, K. Vemaganti, N. Moes, "Hierarchical modeling of heterogeneous solids", Computer Methods in Applied Mechanics and Engineering, 126, 1-16, 172, 3-25, 1999.
[38] T. Strouboulis, L. Zhang, I. Babuska, "p-version of the generalized FEM using mesh-based handbooks with applications to multiscale problems", International Journal for Numerical Methods in Engineering, 60, 1639-1672, 2004.
[39] C. Miehe, "Computational micro-to-macro transitions for discretized micro-structures of heterogeneous materials at finite strains based on the minimization of averaged incremental energy", Computer Methods in Applied Mechanics and Engineering, 192, 559–591, 2003.
[40] I. Temizer, P. Wriggers, "On the computation of the macroscopic tangent for multiscale volumetric homogenization problems", Computer Methods in Applied Mechanics and Engineering, 198, 495–510, 2008.
[41] I.G. Kevrekidis, C.W. Gear, G. Hummer, "Equation-free: The computer-aided analysis of complex multiscale systems", AIChE Journal, 50, 1346–1355, 2004.
[42] G. Samaey, W. Vanroose, D. Roose, I.G. Kevrekidis, "Newton–Krylov solvers for the equation-free computation of coarse traveling waves", Computer Methods in Applied Mechanics and Engineering, 197, 3480–3491, 2008.
[43] Rahul, S. De, "A block preconditioning strategy for Jacobian-free global-local multiscale methods", 9th World Congress on Computational Mechanics (WCCM2010), Sydney, Australia, 2010.
[44] K.J. Bathe, "Finite Element Procedures", Prentice Hall, 1995.
[45] D.H. Allen, "Homogenization principles and their application to continuum damage mechanics", Composites Science and Technology, 61(15), 2223–2230, 2001.
[46] R. Hill, "Elastic properties of reinforced solids: Some theoretical principles", Journal of the Mechanics and Physics of Solids, 11, 357–372, 1963.
[47] Z. Hashin, "Theory of Mechanical Behavior of Heterogeneous Media", Applied Mechanics Reviews, 17, 1–9, 1964.
[48] S. Nemat-Nasser, "Overall Stresses and Strains in Solids with Microstructure", in J. Gittus, J. Zarka, (Editors), "Modeling Small Deformations of Polycrystals", Elsevier Applied Science Publishers, 41–64, 1986.

[49] O. van der Sluis, P.J.G. Schreurs, W.A.M. Brekelmans, H.E.H. Meijer, "Overall behavior of heterogeneous elastoviscoplastic materials: effect of microstructureal modeling", Mechanics of Materials, 32, 449-462, 2000.

[50] K. Terada, M. Hori, T. Kyoya, N. Kikuchi, "Simulation of the multiscale convergence in computational homogenization approach", International Journal of Solids and Structures, 37, 2285-2311, 2000.

[51] V. Kouznetsova, M.G.D. Geers, W.A.M. Brekelmans, "Multi-scale constitutive modelling of heterogeneous materials with a gradient-enhanced computational homogenization scheme", International Journal for Numerical Methods in Engineering, 54, 1235–1260, 2002.

[52] J.E. Dennis, R.B. Schnabel, "Numerical Methods for Unconstrained Optimization and Nonlinear Equations", Prentice- Hall: Englewood Cliffs, NJ, 1983.

[53] Y. Saad, M.H. Schultz, "GMRES: A generalized minimal residual algorithm for solving nonsymmetric linear systems", SIAM Journal on Scientific and Statistical Computing, 7, 856–869, 1986.

[54] P.N. Brown, Y. Saad, "Hybrid Krylov methods for nonlinear systems of equations", SIAM Journal on Scientific and Statistical Computing, 11, 450–481, 1990.

[55] Rahul, S. De, "An efficient coarse-grained parallel algorithm for global–local multiscale computations on massively parallel systems", International Journal for Numerical Methods in Engineering, 82(3), 379-402, 2009.

[56] P. Ladevèze, D. Néron, P. Gosselet, "On a mixed and multiscale domain decomposition method", Computer Methods in Applied Mechanics and Engineering, 196, 1525–1540, 2007.

[57] K. Matsui, K. Terada, K. Yuge, "Two-scale finite element analysis of heterogeneous solids with periodic microstructures", Computers and Structures, 82, 593–606, 2004.

[58] P. Eder, J. Giuliani, S. Ghosh, "Multilevel parallel programming for three-dimensional Voronoi cell finite element modeling of heterogeneous materials", International Journal of High Performance Computing Applications, 19, 29–45, 2005.

[59] P. Eder, J. Giuliani, S. Ghosh, "Multi-level parallel programming for multi-scale adaptive finite element modeling of heterogeneous materials", International Journal of Multiscale Computational Engineering, 2, 421–443, 2004.

[60] C. Vandekerckhove, I. Kevrekidis, D. Roose. "An efficient Newton-Krylov implementation of the constrained runs scheme for initializing on a slow manifold", Journal of Scientific Computing, 39, 167–188, 2009.

[61] K. Burrage, J. Erhel, B. Pohl, "Restarted GMRES preconditioned by deflation", Journal of Computational and Applied Mathematics, 69, 303–318, 1996.